ISSN 1075-7015, Geology of Ore Deposits, 2018, Vol. 60, No. 6, pp. 527–545. © Pleiades Publishing, Ltd., 2018.
Original Russian Text © A.V. Volkov, N.E. Savva, E.E. Kolova, V.Yu. Prokofiev, K.Yu. Murashov, 2018, published in Geologiya Rudnykh Mestorozhdenii, 2018, Vol. 60, No. 6, pp. 590–609.

Dvoinoe Au–Ag Epithermal Deposit, Chukchi Peninsula, Russia

A. V. Volkov[a, *], N. E. Savva[b], E. E. Kolova[b], V. Yu. Prokofiev[a], and K. Yu. Murashov[a]

[a] *Institute of Geology of Ore Deposits, Petrography, Mineralogy, and Geochemistry, Russian Academy of Sciences, Moscow, 119017 Russia*

[b] *Northeast Interdisciplinary Science Research Institute, Far East Branch, Russian Academy of Sciences, Magadan, 685000 Russia*

**e-mail: alexandr@igem.ru*

Received February 17, 2017

Abstract—The Dvoinoe Au-Ag low-sulfide epithermal deposit is located in the Ilirnei ore district (western Chukotka) within the outer zone of the Okhotsk–Chukotka volcanic belt (OChVB). The paper considers the results of geological–structural, mineralogical–geochemical, and thermobarogeochemical studies of the deposit. The ores of the deposit are characterized by dominant colloform-banded (often combined with brecciated) structures; a high Au/Ag ratio (1 : 1 to 1 : 2); low sulfidity (<0.5%); the presence of hessite, small sulfide segregations (0.005–0.015 mm), and a larger amount of native gold (0.01–0.07 mm); high Au, Ag, and Sb contents; relatively high As, Cu, Pb, and Cd contents; higher Zn, Bi, and Te contents; a low total REE; and negative Eu and positive Ce anomalies. The geochemical features are consistent with the ore mineral composition. The high Rb/Sr, Th/La, Y/Ho, and U/Th ratios of ores are most likely caused by the position of the deposit in the zone of influence of the Ilirnei granitic pluton. A fluid inclusion study showed that the ores were formed from Na–K–Mg low-saline (5.58–0.2 wt % NaCl-equiv.) hydrothermal fluids with a small amount of CO_2, H_2S, and CH_4 with decreasing temperatures from 370 to 130°C and the following fluid parameters: CO_2/CH_4 = 217–53, Na/K = 5–2, and K/Rb = 2722–202. The results are compared with original and published data on the Kupol, Moroshka, and Sentyabr'sky deposits. Our data are important for regional forecasting, interpreting metallogeny, and the search for and evaluation of Au–Ag epithermal deposits.

Keywords: western Chukotka, deposit, epithermal, ore mineralogy, gold, silver, trace elements, fluid inclusions, genetic features

DOI: 10.1134/S1075701518060053

INTRODUCTION

The Dvoinoe deposit is located in the Chaun district of the Chukotka Autonomous Okrug (CAO) 130 km east of the town of Bilibino and 300 km (by winter automobile road) from the nearest seaport Pevek (Fig. 1, inset). The deposit was discovered by the Anyui Geological Prospecting Expedition as a result of geochemical survey of dispersion trains on a 1 : 200000 scale. Geological prospecting works ended before 1991. Later (1993), the deposit, with reserves of ~9 t (47.3 g/t Au, on average) to a depth of 100 m from the surface, was purchased by the Severnoe Zoloto Company. From 1996 through 2007, ~8 t of gold were extracted in an open pit at the deposit.

In 2007, the deposit was purchased by the Millhouse Company, which completed detailed exploration of ore zones (nos. 37 and 38) and defended the reserves in the State Commission on Reserves of the Russian Federation (64 t of gold and 94 t of silver with average contents of 18.6 and 27.0 g/t Au and Ag, respectively). In 2010, the deposit, along with adjacent Vodorazdelny district, passed to the Kinross Gold Corporation. This company built a new mine, commissioned in October 2013 with projected underground production of up to 1 Mt of ore per year; the ore is delivered by an automobile road to the gold recovery plant of the Kupol mine 100 km to the south.

According to data of the CAO administration, the deposit produced 10.5 t of gold and 16.8 t of silver in 2016. A significant increase in reserves is expected due to recent detailed exploration of deep horizons of ore zone no. 1.

Since the moment of their discovery, the geological structure and composition of ores of the deposit have been studied by the Northeastern Branch of the Central Research Institute of Geological Prospecting for Base and Precious Metals (TsNIGRI) (Volkov et al., 2006). In 2011–2012, fluid inclusions in quartz from ore zone nos. 1 and 37 were studied at the Institute of Geology of Ore Deposits, Petrography, Mineralogy, and Geochemistry, Russian Academy of Sciences (IGEM RAS) (Volkov et al., 2012; Prokofiev et al., 2012). In 2014–2016, studies of the mineralogical–geochemical and thermobarogeochemical features of ores were supported by the Russian Science Foundation (project no. 14-17-00170) and were continued in

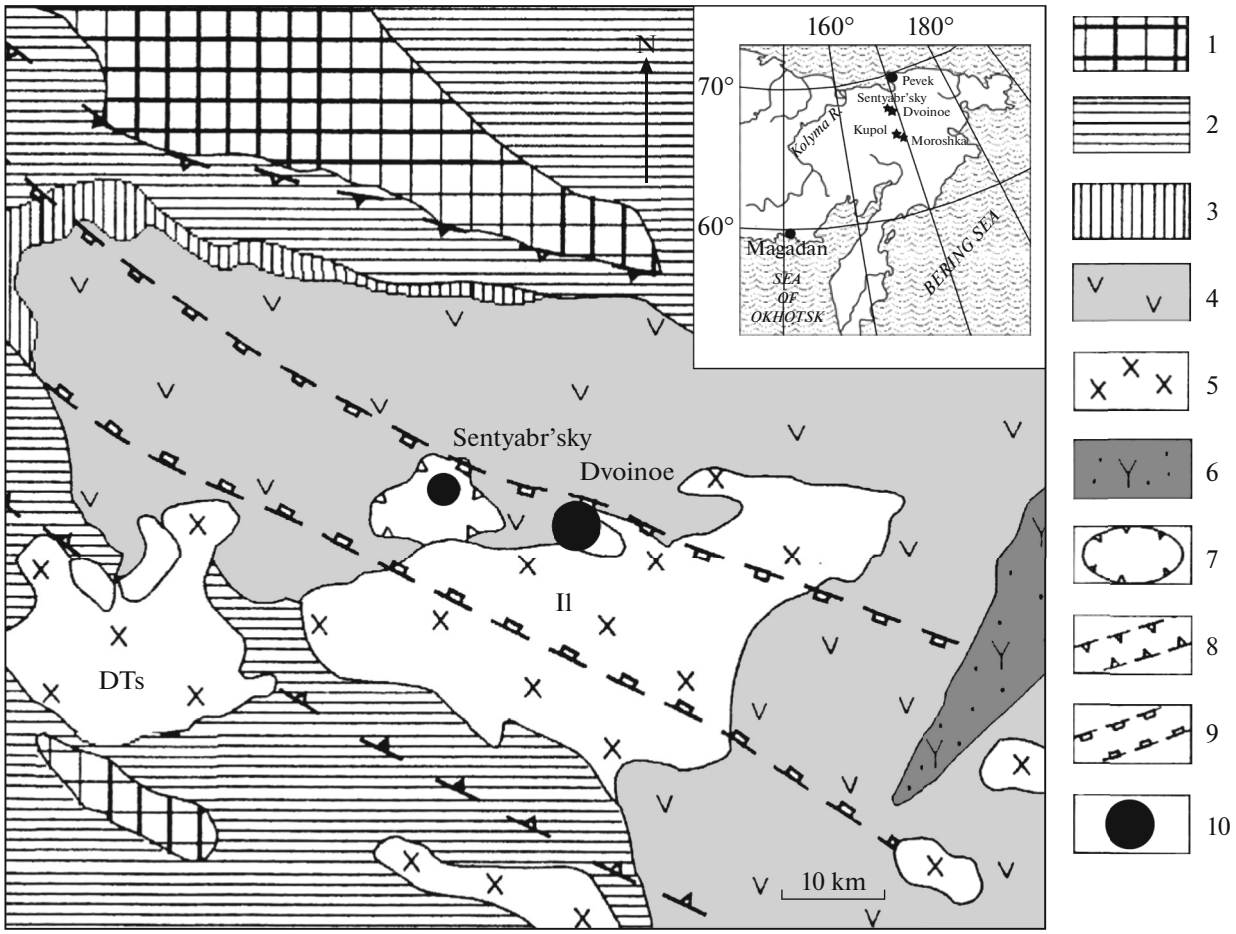

Fig. 1. Location of Dvoinoe deposit in regional structures, modified after (Volkov et al., 2006). (1, 2) Lower structural stage: (1) Keperveem Formation, schist complex; (2) flyschoid complex; (3, 4) upper structural stage: (3) terrigenous–carbonate complex; (4) rhyolite–dacite complex; (5) Early Cretaceous intrusions; (6) Late Cretaceous subvolcanic bodies; (7) Ilirnei volcanic structure; (8) Keperveem deep fault zone; (9) Early Cretaceous Tytliutin fault zone; (10) epithermal Au–Ag deposits; Il, Ilirner pluton; DTs, Dva Tsirka pluton.

2017–2018 with the support of the Presidium of the Russian Academy of Sciences (program no. 4). Studying the composition and parameters of ore-forming fluids to identify their origin has been of the key problems in the theory of endogenic ore formation for many decades (Bortnikov et al., 2006).

ANALYTICAL METHODS

The mineral composition of ores was studied on an Axioplan Imaging optical microscope. The composition of ore minerals was analyzed on a Camebax microprobe equipped with an INCA Camebax device (analyst T.V. Subbotnikova). We studied core samples from boreholes that exposed ore zone no. 37 at various depths.

The geochemical features of ores were studied at the Analytical Laboratory of IGEM RAS. The contents of major oxides and certain trace elements were analyzed by X-ray fluorescence on an Axios mAX wavelength dispersive vacuum spectrometer (PANalytical, the Netherlands, 2012, www.panalytical.com). The spectrometer was calibrated against branch and state standard samples of rock chemical compositions. The analysis was conducted following the method of 439-RS NSAM VIMS providing results by OST RF 41-08-205-04 (analyst A.I. Yakushev). Trace element contents were measured on an X-Series II mass spectrometer with inductively coupled plasma (analyst Ya.V. Bychkova). The detection limits of elements varied from 0.1 ng/g for heavy and middle elements up to 1 ng/g for light elements. The analytical error is 1–3 rel %. The Au content was analyzed on a Spectr AA220Z atomic absorption spectrometer with electrothermal atomization (analyst V.A. Sychkova). The results were compared with trace and rare earth element contents of host volcanic rocks of the Okhotsk–Chukotka volcanic belt (OChVB) (Tikhomirov et al., 2008, 2016; Sakhno et al., 2015). The geochemical indicators were determined to estimate the formation conditions of

epithermal Au-Ag deposits. The results have been tabulated and were the basis for REE and other trace element patterns of ores from the deposit.

Cryothermometric fluid inclusion (FI) studies (n = 218) were carried out on measurement apparatus including a THMSG-600 system (Linkam, Great Britain), Amplival (Germany) and Motic (China) microscopes, a video camera, and a computer. The salinity of FIs was calculated from ice melting temperature ($T_{\text{ice melting}}$) after (Bodnar and Vityk, 1994). The salt composition of fluids was estimated from eutectic temperatures (Borisenko, 1977). The salinity and pressure of water vapor were estimated in the FLINCOR program (Brown, 1989). The bulk composition of FIs was studied at the Analytical Laboratory of TsNIGRI (analyst Yu.V. Vasyuta) using gas and ion chromatography and ICP MS following (Kryazhev et al., 2006).

The Raman spectroscopy of FIs was carried out at the Laboratory of Thermobarogeochemistry of the Institute of Geology and Mineralogy, Siberian Branch, Russian Academy of Sciences (IGM SB RAS, Novosibirsk) on a Lab Ram HR 800 Raman spectrometer in a wide spectral range of 150–3800 cm^{-1}, the 532 nm excitation line of a He–Ne laser, and an aperture diffraction width of 1800 cm^{-1} (analyst E.E. Kolova). The composite contours were broken down in the Origin 7.5 program.

FEATURES OF THE GEOLOGICAL STRUCTURE OF THE DEPOSIT

The Dvoinoe deposit is localized in the Ilirnei volcanic structure, in the central part of the Tytyl'veem Trough of the OChVB (Fig. 1). This trough is confined to the axial, most depressed part of the Upper Nomnunkuveem Syncline of the Anyui fold zone (Fig. 1). The trough (90 × 40 km) is characterized by a striking two-storied structure. The lower horizons (marine molasse) consist of sandy-clayey and carbonate rocks, and the upper horizons, of rocks of rhyolite-dacite and porphyritic assemblages. The central part of the trough is mostly filled with pyroclastic rocks.

The deposit is situated on the eastern flank of the Ilirnei caldera bounded by the eponymous granitic pluton (Fig. 1). The oval (14 × 6 km) caldera is bounded by arch adjacent faults steeply (75°–80°) dipping toward the center of the structure. The ore field of the deposit, in an area of ~20 km^2, consists of Aptian andesites and andesitic tuffs (the $^{40}Ar/^{39}Ar$ age is 120–118 ± 1 Ma) (Akinin et al., 2015; Sakhno et al., 2015). The ore-hosting rocks are inclined, dipping to the northwest at angles of 10°–40°. The thickness of the tuffaceous horizons is 10–130 m. Dark gray small porphyritic andesites belong to the K–Na series (Na_2O/K_2O = 1.1).

The Ilirnei granitic pluton is a complex igneous body elongated to the northwest (Fig. 1) with rocks of two intrusion phases. Earlier granites and granodiorites developed along its periphery. Several stocks of leucocratic granites are assumed to occur in the central part of the pluton.

According to geophysical data, the Dvoinoe deposit is located in the zone of influence of the Ilirnei pluton and Dva Tsirka intermediate–mafic intrusive. The latter has an ellipsoid morphology and extends northeast for 14–15 km with a width of 6–7 km. In cross section, it is characterized by a laccolith morphology and has a thickness of 1.0–1.5 km. The interaction zone of both plutons, saturated with dikes and sills, was probably the most permeable and favorable for ore deposition.

NE- and NW-trending dikes of mostly porphyry granites are elongated (800–1700 m), thick (up to 45 m), steeply dipping bodies with curve contours and numerous apophyses. Thin (0.5–2.4 m) basalt dikes occur in the deep horizons of the deposit, where they form fanlike pockets. The porphyry granite dikes are preore, whereas the basalt dikes are pre- and intraore (Volkov et al., 2006).

The northwestern fault zone is the main ore-controlling and ore-hosting structure, with all the orebodies of the deposit (Fig. 1). The zone dips to the northeast at angles of 60°–90°. We suggest that tuffaceous horizons lithologically controlled the mineralization. The deposit includes 13 ore-bearing stringer zones, four of which are economically important and have been studied in various degrees of detail.

The veins and veinlets are composed of quartz–chalcedony aggregates (80–90%), adularia (5–7%), carbonates (up to 5%), pyrophyllite, and chlorite. The Au and Ag distribution in orebodies is extremely nonuniform: the Au and Ag contents reach 3300 and 16300 g/t, respectively, and their variation coefficients attain 376 and 632%, respectively. Mineralization is characterized by low sulfidity (<1%) and a low Au/Ag ratio (1 : 1 – 1 : 2).

The productivity of ores is caused by the presence of native gold with low fineness, which mostly occurs in vein colloform-zonal quartz with small xenoliths of host rocks. This is the main mode of its occurrence in ores. A minor amount of Au is hosted in acanthite, hessite, and low-Ag fahlores. Approximately 90% of Au and Ag reserves of the Dvoinoe deposit are concentrated in ore zone nos. 1 and 37.

Ore zone no. 1, which has a longitudinal strike and steep (70°–80°) northeastern dip, is confined to the contact of a thick porphyry granite dike (Fig. 2a). The total length of the zone is 1400 m (the productive part is 400 m) with a thickness of 25–30 m. The vertical scale of the ore pipe is more than 350 m. The main Au and Ag reserves are confined to the hanging wall contact. The zone includes three morphological areas. The northwestern and southeastern areas have ore shoots with several parallel veins and numerous apophyses 200–250 m long with a total thickness of up

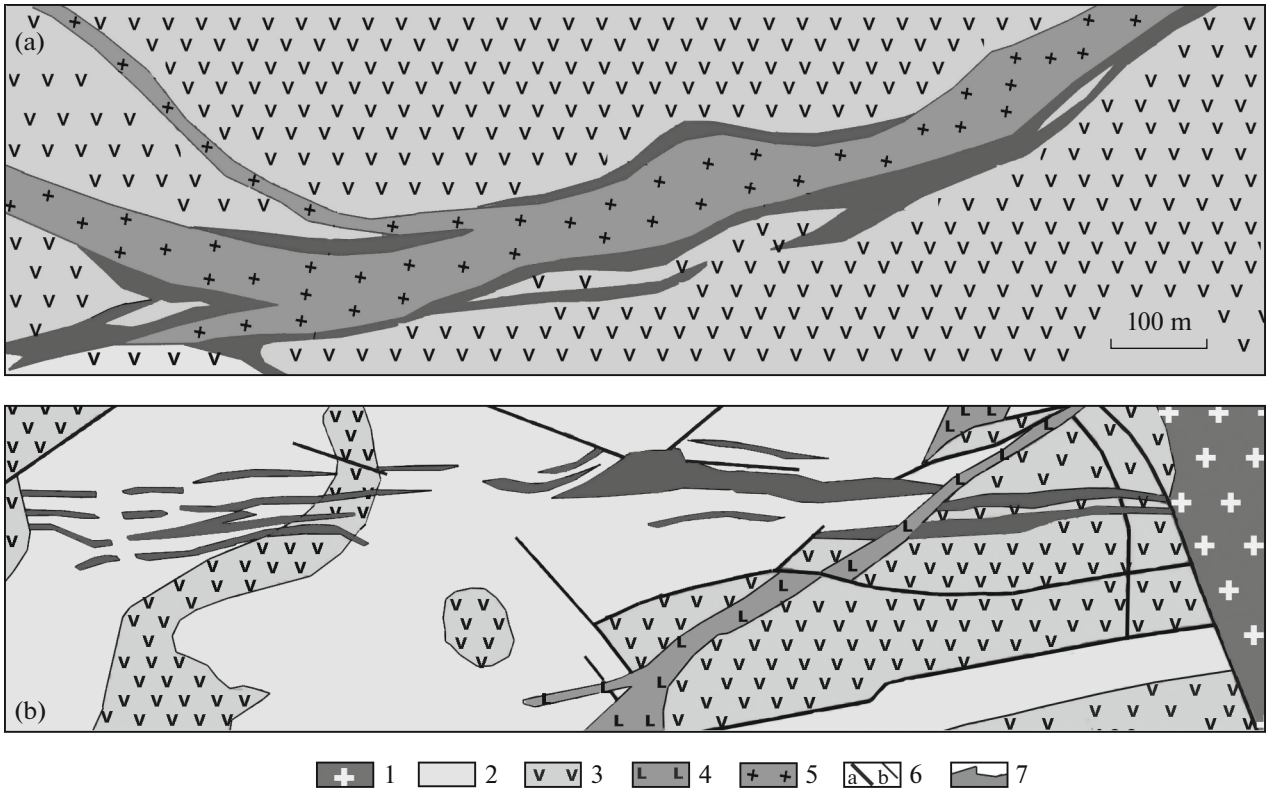

Fig. 2. Geological plan of ore zones no. 1 (a) and no. 37 (b) of Dvoinoe deposit, modified after materials of Severnoe Zoloto Company. (1) Granites of Ilirnei pluton; (2) dacites; (3)andesites, their tuffs; (4) quartz porphyry syenite dike; (5) porphyry granite dike; (6) faults (a), geological boundaries (b); (7) epithermal Au–Ag-bearing veins and ore columns.

to 23 m (8 m, on average) and high Au and Ag contents. The central area is associated with a dike swell and is a thin (up to 2.5 m) veinlet zone.

Ore zone no. 37 consists of a system of stringer bodies (Fig. 2b) and is poorly eroded: only a small area (20 × 30 m) is exposed on a slope with heights of +1015 to +1025 m. Almost the entire extent of the ore zone in the surface is accompanied by a thick (up to 100 m) NE-striking band of hydrothermal–metasomatic alteration. Drilling has shown that the zone is more than 940 m long. It generally dips to the southwest. In the northern flank, it is shielded by felsic volcanic rocks of an intermediate sequence. The thickness of the zone varies from several to 30 m or more in the central ore shoot. The overall vertical scale is more than 350 m (including sills). The ore zone becomes gentler at depth (up to 70°). The zone hosts two thick main veins located inside a linear stockwork of variable thickness. The central ore pipe bears most of the Au and Ag.

Ore formation was preceded by regional low- and middle-temperature propylitic alteration under alkaline conditions genetically related to the origination of granitic rocks. Potassium feldspar is the most abundant mineral, hydromica is subordinate, and epidote and pyrophyllite are minor. The fractures are filled with quartz-carbonate aggregates. The rocks host disseminated sulfides (~3%).

STRUCTURAL FEATURES OF ORES

Ore zone nos. 1 and 37 are characterized by dominant colloform-banded (often with brecciated) ore structures (Fig. 3), which indicate ore formation accompanied by tectonic activity. The colloform-crustification veins exhibit rhythmically banded deposition of quartz, adularia, carbonates, and hydromica (Figs. 3b–3e). The boundary between quartz and hydromica bands host ore minerals that impart a dark color to the bands and form typical ginguro structures (Figs. 3b, 3e). Aggregates of ore minerals are characterized by small-grained cementation textures, rare emulsion exsolution textures, and rim replacement textures. The ore minerals form finely dispersed, unevenly pocketed, banded, and lenticular disseminations responsible for disseminated, spotty, and vaguely banded ore structures (Figs. 4a, 4b). The breccias host fragments of metasomatically altered host rocks (rhyolites, andesites, their tuffs). The matrix is composed of quartz–adularia–carbonate–hydromica aggregate with fine ore dissemination (Fig. 4c). The structural zoning is typical of epithermal Au–Ag deposits of the OChVB (Sidorov, 1978).

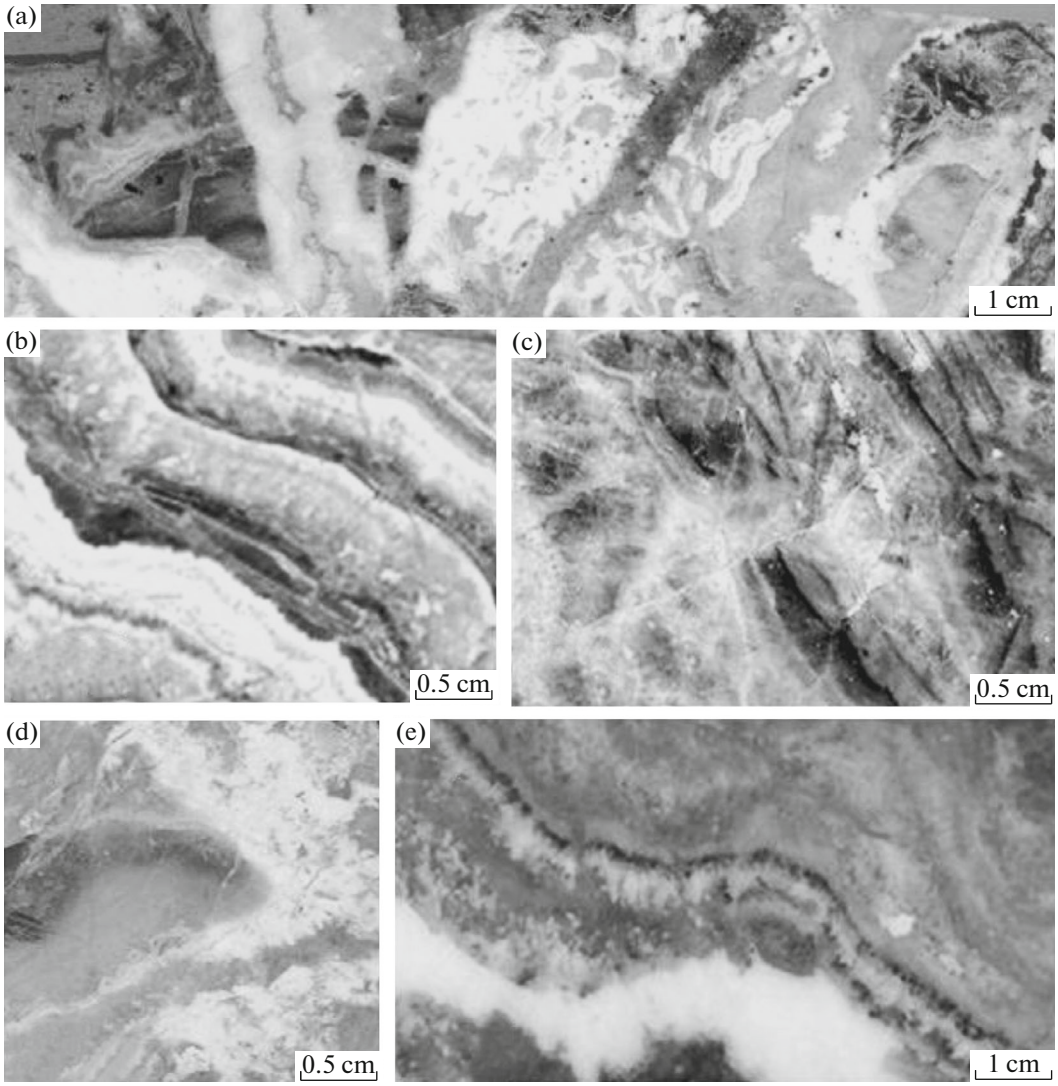

Fig. 3. Combination of brecciated and colloform-banded structures of Dvoinoe deposit (ore zone no. 37): (a) quartz–adularia material cementing chloritized fragments of host rocks; (b) colloform-banded structure (rhythmic intercalation of quartz–adularia–chlorite–hydromica bands); (c) fractured chlorite layers; (d)–(e) colloform-banded structure of quartz–adularia–chlorite–hydromica aggregate.

MINERALOGICAL FEATURES OF ORES

The poorly diverse ores from the deposit are characterized by small sizes of ore minerals (mostly, 0.005–0.015 mm) and their close aggregates. Fifty-three minerals have been identified in ores (Table 1). The main ore minerals include native gold, pyrite, chalcopyrite, galena, and sphalerite with subordinate acanthite and fahlores. The gangue minerals are quartz, adularia, and calcite with subordinate epidote, hydromica, sericite, muscovite, chlorite, biotite, albite, etc. Below we describe the main gangue and ore minerals.

Quartz is inequigranular mostly small-grained to chalcedony and locally forms larger crystals (2–3 mm across). It makes up bands 1–3 cm thick and spotty aggregates and is characterized by a high amount of FIs (Fig. 4d). The ore mineralization is also confined to bands of FI-saturated small-grained quartz and adularia–hydromica aggregate.

White *carbonates* (probably calcite) form pockets and veinlets up to 8 mm thick in quartz. Minor ferrous yellowish brown carbonates (probably ankerite) occur as spotty (locally, spherical) aggregates intergrown with hydromica up to 5 cm in quartz bands.

Chlorite (0.1–1.0%) forms fine-scaly aggregates along with hydromica. Its optical properties correspond to clinochlore.

Adularia comprises rhythmic bands at the boundary with small-grained quartz (Fig. 4a). It is intensely replaced by hydromica. Its grain size is <0.5 mm.

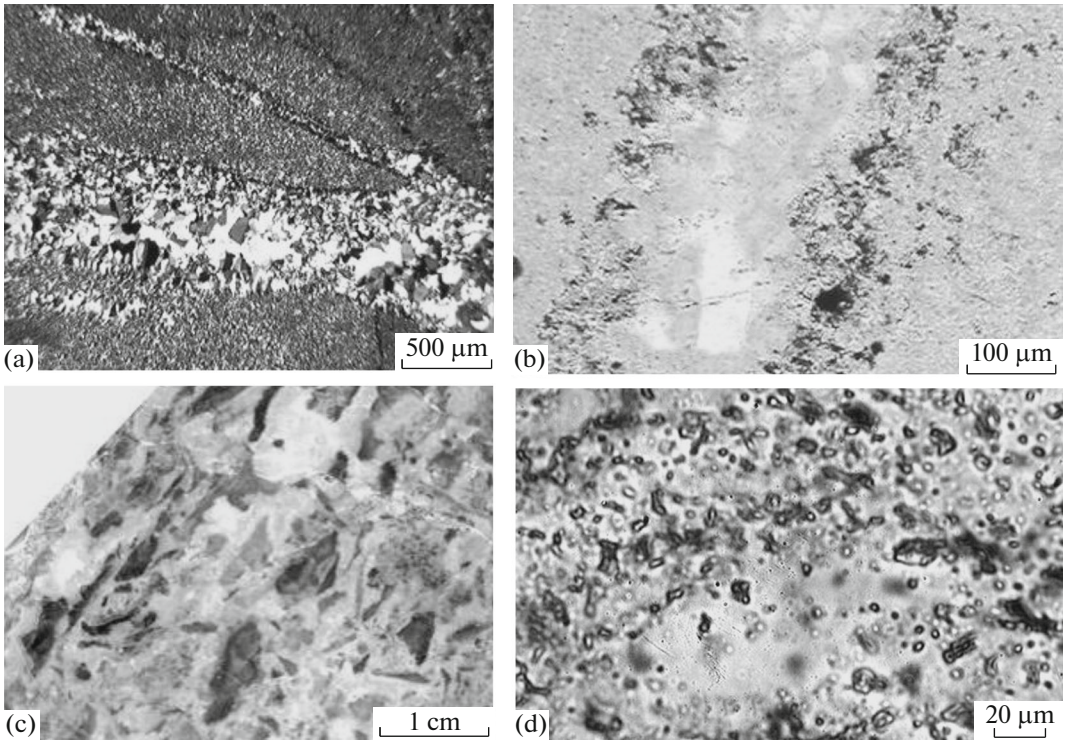

Fig. 4. Textural–structural features of ores from Dvoinoe deposit: (a) structure of quartz–adularia bands (without analyzer); (b) fine ore dissemination in chlorite–hydromica aggregate; (c) breccia with pyrophyllite–hydromica clasts in quartz matrix (ore zone no. 37); (d) pink quartz saturated with fluid inclusions (ore zone no. 37).

Pyrophyllite locally occurs in breccias, where it almost completely replaces rock fragments and is associated with quartz, calcite, and small amount of chlorite (Fig. 4c). The mineral has been identified on a TERMOSCAN device.

Pyrite forms individual crystals and intergrowths thereof 0.1–0.8 mm in size with inclusions of galena and low-fineness gold. It is variously brecciated and cemented by galena, sphalerite, chalcopyrite, and fahlore. The mineral is stoichiometric and contains a minor amount of Cu.

Sphalerite forms anhedral segregations 0.03–1.2 mm in size in chalcedony quartz. It is characterized by uneven color with colorless ideally transparent areas along grain peripheries. Transparent cleiophane also frequently occurs (Table 2). Fe-bearing (0.24–0.57 wt % Fe) sphalerite hosts emulsions of chalcopyrite and local inclusions of native gold.

Native gold occurs mostly in vein colloform-zonal quartz with small xenoliths of host rocks. Microscopic inclusions of native gold are also observed in carbonate, pyrite, sphalerite, fahlore, hessite, galena, and

Table 1. Mineral composition of ores from Dvoinoe deposit

Groups of minerals	Major	Subordinate	Rare
Gangue	Quartz, calcite, adularia, hydromica	Chalcedony, pyrophyllite, ankerite, titanite, amphibole, chlorite, epidote, sericite, muscovite	Barite, leucoxene, kaolinite, apatite, zircon, actinolite, biotite, garnet, zeolite, moissanite, periclase, albite, prehnite, rutile, ilmenite
Ore	Pyrite, sphalerite, chalcopyrite, galena, native gold	Electrum, hessite, tennantite-tetrahedrite, cleiophane, acanthite, magnetite, hematite, marcasite	Goldfieldite, pearceite, jalpaite, titanomagnetite, cassiterite, anglesite, cerussite, covelline, chalcocite, malachite, azurite, jarosite

The table takes into account the unpublished data of A.P. Epifanova (1990).

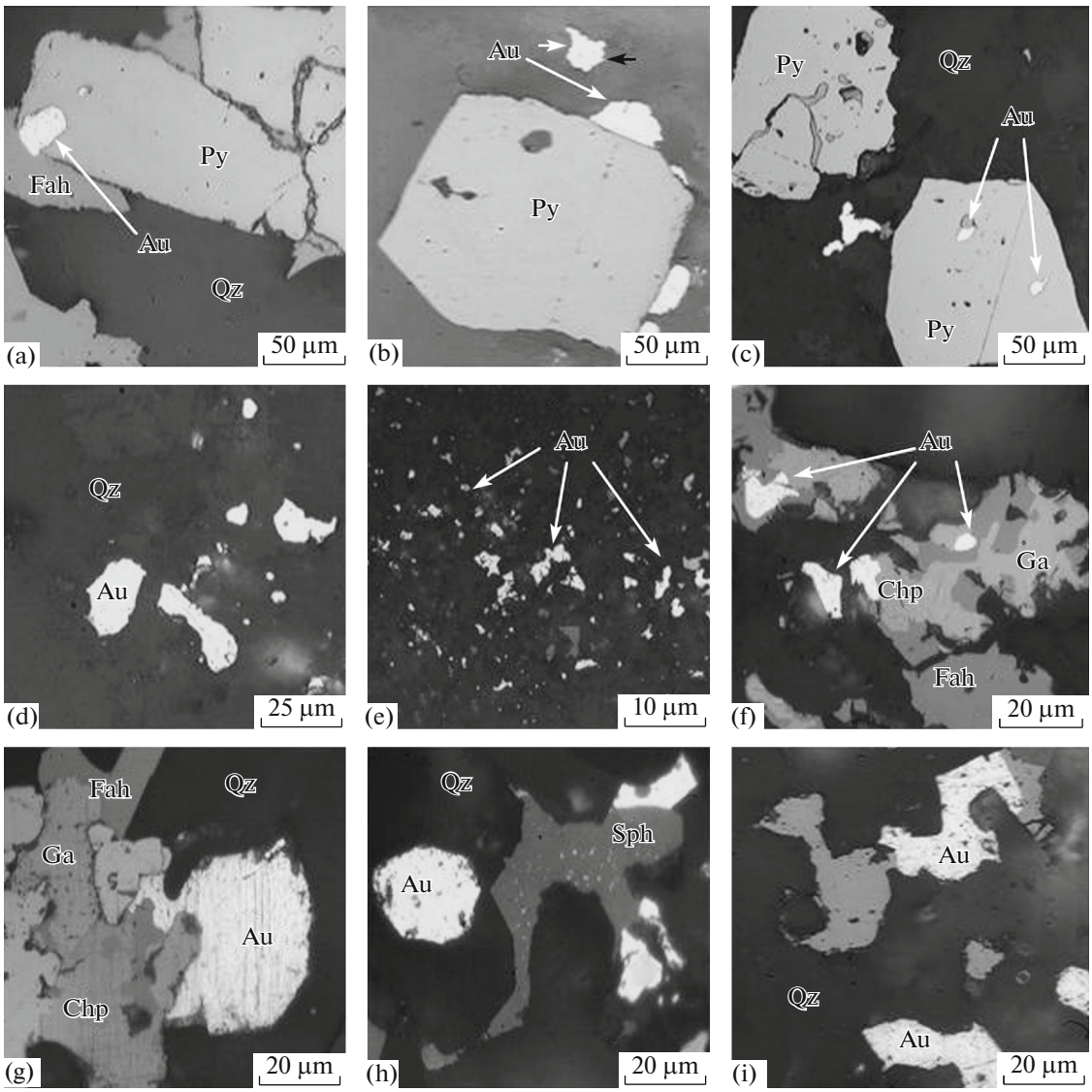

Fig. 5. Microscopic gold in ores from Dvoinoe deposit: (a–c) gold intergrown with pyrite; (d, e) gold in quartz; (f, g) gold intergrown with chalcopyrite and fahlore; (h) gold monocrystal in quartz and intergrowth of gold and sphalerite; (i) free gold in quartz and gold intergrown with galena.

chalcopyrite or scaly accumulations in chalcedony–hydromica aggregate as saturated bands and spots (Fig. 5). The gold grain size varies from hundredths of a millimeter up to 1 mm (larger grains are rare); the fineness of gold is 725–776‰ (Table 2). The gold grains are characterized by veinlet, interstitial, scaly, film, wire, and flat dendrite morphology (Fig. 5).

Acanthite is a major Ag-bearing mineral. It is mostly intergrown with galena and fahlore and rarely occurs as individual grains. Under a microscope it is observed as small interstitial grains in quartz.

Hessite forms droplike inclusions in fahlore (Fig. 6). It is identified by its optical properties (pinkish yellow color, high anisotropy) and microprobe analysis (Table 2).

Fahlore (tennantite–tetrahedrite) (Table 2) forms interstitial aggregates (Fig. 6) and euhedral crystals. It frequently rims galena grains and is intergrown with native gold, galena, sphalerite, chalcopyrite, and hessite. It is characterized by low Ag (0.00–1.64 wt %) and variable As, Sb, Fe, and Zn contents (Table 2).

Galena heals cataclasis fractures in pyrite. The mineral has been found as subhedral aggregates 10–70 μm in size in quartz (Fig. 6). Galena is covered by acanthite films. It also occurs in close association with chalcopyrite and sphalerite. The composition of galena is close to stoichiometric and is characterized by stable Se (0.81–5.17 wt %) and rare Sb (1.97 wt %) contents (Table 2).

Table 2. Chemical composition of ore minerals from Dvoinoe deposit (wt %)

S	Fe	Cu	Zn	As	Se	Ag	Sb	Au	Pb	Total
Chalcopyrite										
35.42	30.67	35.76								101.85
35.98	30.69	35.51								102.17
35.61	30.46	35.38								101.46
Tennantite-tetrahedrite										
27.92	2.77	42.19	5.24	14.02			9.64			101.79
27.42	2.60	41.85	5.76	12.50			11.67			101.8
27.51	2.36	39.95	4.91	12.91			10.19			97.68
26.23	2.25	39.85	5.37	8.24		1.20	17.03			100.16
26.34	2.16	39.78	5.48	8.73		1.14	16.81			100.45
28.11	2.55	41.55	5.60	13.89			8.95			100.66
27.14	2.41	41.08	5.63	13.78			9.69			99.74
25.4	1.76	38.34	5.87	4.38		1.64	22.34			99.73
Se-bearing galena										
12.53		1.63			1.49				86.53	102.18
12.77		1.47			1.44				87.32	102.99
12.48		0.76			0.95				83.45	97.64
12.07		1.14			0.81				84.26	98.27
12.75		1.08			0.81				86.08	100.72
Low-fineness native gold										
						28.49		72.54		101.03
						23.56		77.62		101.18
						26.56		74.23		100.78
						24.33		76.52		100.85
						24.80		75.67		100.48
						27.57		72.72		100.28
Fine mineral mixture of fahlore and electrum										
20.8	4.93	20.11	3.75	6.78		13.55	6.36	24.36		100.64
Sphalerite										
33.02			63.32							97.55
33.45			66.15							99.60
Hessite										
S	Fe	Cu	Zn	As	Se	Ag	Sb	Au	Te	
						63.68			37.64	101.32
		0.64				64.11			37.6	102.35
Goldfieldite + hessite (mixture)										
7.27	0.64	12.7	2	1.35		42.61	7.57		25.4	99.53
14.94	1	23.7	3.72	2.22		25.48	16.16		13.49	100.7

*, Camebax microprobe equipped with Inca device, analyst T.V. Subbotnikova (SVKNII FEB RAS).

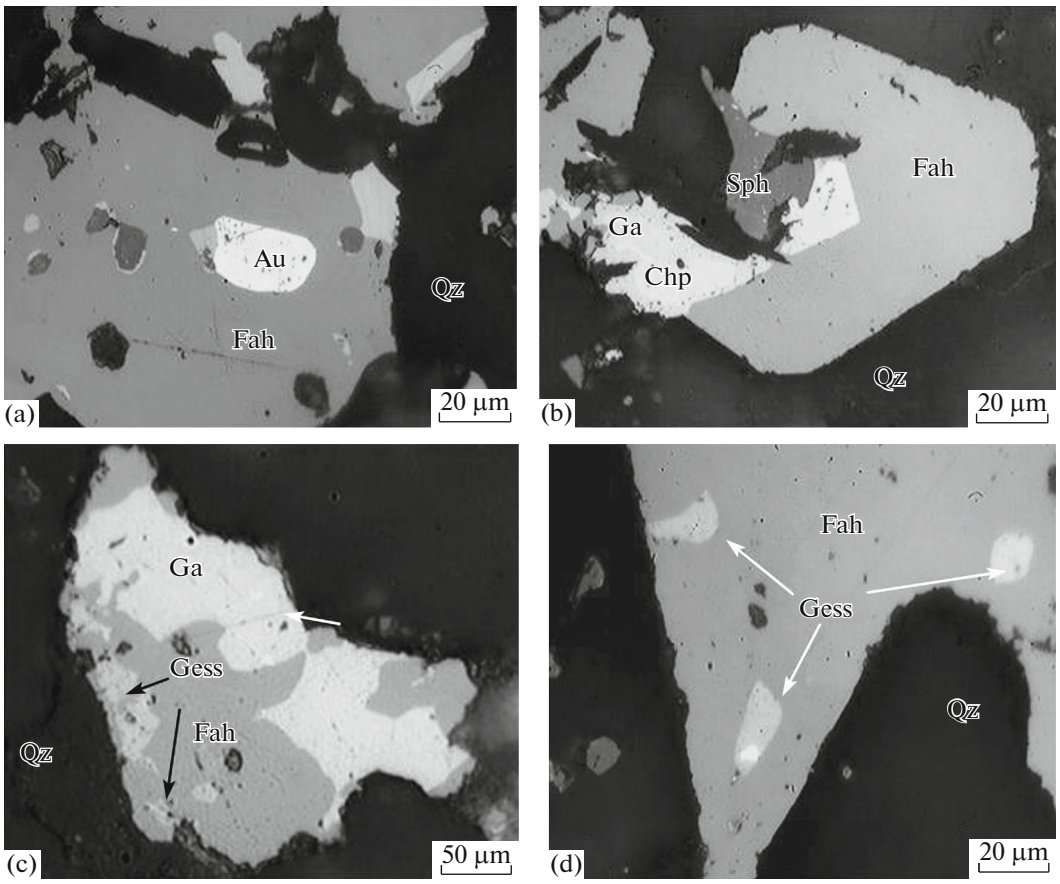

Fig. 6. Aggregates of ore minerals: (a) inclusion of native gold in fahlore; (b) euhedral grain of fahlore intergrown with galena, sphalerite, and chalcopyrite; (c) intergrowth of fahlore, hessite, and galena; (d) inclusion of hessite in fahlore.

Thus, the major features of ores from the Dvoinoe deposit include low sulfidity (<0.5%), the presence of hessite (Ag_2Te), small sulfide grain sizes (mostly, 0.002–0.015 mm, rarely up to 1 mm), fine-grained native gold (0.01–0.07 mm, locally, 0.1–0.2 mm), ~50% of native gold intergrown with sulfides, and the remaining "free" gold as grains in quartz and quartz–hydromica aggregates.

FLUID INCLUSION STUDY RESULTS

One hundred twenty FIs in quartz from two surface samples from ore zone no. 37 were studied at IGEM RAS. Ninety-eight FIs in quartz of three samples from ore zone no. 1 and two samples from ore zone no. 37 and sphalerite of one sample from ore zone no. 37 taken from different depths of drill core were studied at the Northeast Interdisciplinary Science Research Institute, Far East Branch, Russian Academy of Sciences (Table 3). Primary and primary–secondary FIs 2–31 μm in size were selected for microthermometry studies. The FIs at room temperature are two-phase with a vapor and a liquid (aqueous salt solution) (Fig. 7). Primary and primary–secondary FIs 20–15 μm in size suitable for microthermometry studies were found in medium-crystalline productive quartz from ore zone nos. 1 and 37. At room temperature, the FIs are two-phase with a vapor and a liquid (aqueous salt solution) (Fig. 7). The FIs are elongated (rarely round) and are unevenly distributed (mostly along the growth zones, rarely in groups). The elongated FIs in sphalerite occur as minor groups along cleavage planes.

The FIs in quartz of ore zone nos. 1 and 37 and sphalerite are homogenized at temperatures of 130–325, 133–300, and 362.5–370°C, respectively (Table 3, Fig. 8). According to cryometric studies, $T_{ice\ melting}$ of all FIs ranges from –3.6 to –0.1°C corresponding to a salinity of 5.86 to 0.2 wt % NaCl-equiv. Judging from the eutectic temperatures (–36 to –21°C), the composition of solutions is dominated by Na and K chlorides with a subordinate amount of Mg and Fe chlorides. The calculated fluid density increased from 0.70 to 0.95 g/cm^3 with decreasing temperature.

The Raman spectroscopy of vapor phases ($n = 8$) of FIs in quartz of ore zone no. 1 (samples from depths of 37–39 and 43–44 m, T_{hom} = 279–230°C) showed the presence of low-density CO_2 and CH_4 and a minor amount of gases of the HS^- group (Fig. 9).

Table 3. Results of microthermometry studies of individual fluid inclusions in sphalerite and quartz of ore veinlets from the Dvoinoe epithermal Au–Ag deposit

No.	*n*	T_{hom}, °C	T_{eut}, °C	$T_{ice\ melting}$, °C	*C*, wt % NaCl-equiv.	Density, g/cm^3	Source
Sphalerite							
1	5	325–370	–22 to –26	–0.1 to –1.2	0.2–2.1	0.55–0.63	New data
Quartz							
2	9	285–320	–23 to –26	–0.1 to –1.0	0.2–1.7	0.64–0.73	New data
3	4	259–279	–23 to –26	–0.1	0.2	0.73–0.77	
4	9	202–247	–23 to –29	–0.1 to –1.5	0.2–2.6	0.80–0.88	
5	12	143–178	–23 to –29	–0.1 to –1.5	0.2–2.6	0.90–0.94	
6	9	130–140	–22 to –24	–0.1 to –3.6	0.2–5.9	0.92–1.05	
7	9	273–300	–21 to –26	–0.1 to –2.0	0.2–3.4	0.7	
8	7	164–224	–24	–0.1 to –1.8	0.2–3.1	0.83–0.90	
9	7	251	–27	–0.8	1.4	0.80	Volkov et al., 2012; Prokofiev et al., 2012
10	6	216	–29	–2.9	4.8	0.89	
11	6	203	–33	–3.0	5.0	0.90	
12	4	202	–28	–0.1	0.2	0.87	
13	3	173	–31	–0.3	0.5	0.90	
14	3	172	–30	–3.0	5.0	0.95	
15	3	154	–32	–2.5	4.2	0.95	
16	2	248	–34	–0.3	0.5	0.80	Nikolaev et al., 2013
17	3	233	–32	–0.6	1.1	0.83	
18	2	226	–36	–0.7	1.2	0.84	
19	3	204	–27	–1.7	2.9	0.89	
20	3	200	–36	–2.3	3.9	0.90	
21	2	184	–28	–1.7	2.9	0.91	
22	3	181	–30	–0.9	1.6	0.90	
23	3	163	–31	–0.3	0.5	0.91	
24	3	160	–27	–1.7	2.9	0.93	
25	6	133	–30	–1.4	2.4	0.95	
26	4	209	–28	–0.5	0.9	0.86	
27	3	173	–27	–0.3	0.5	0.90	
28	3	162	–27	–0.4	0.7	0.92	
29	6	153	–28	–0.6	1.1	0.93	

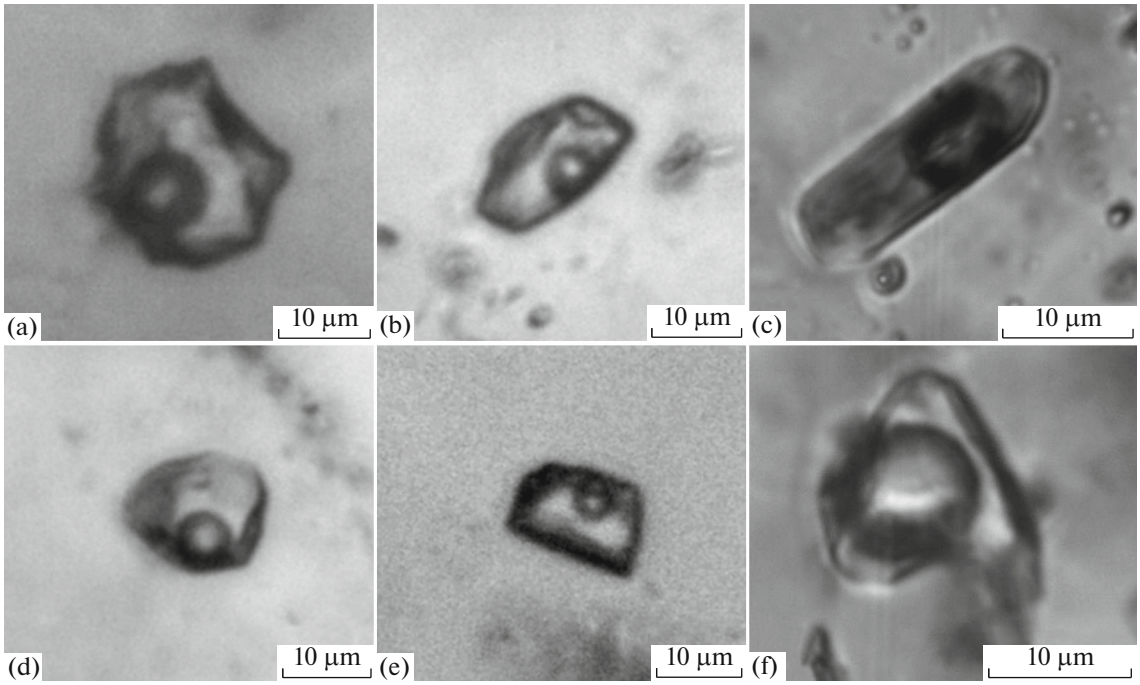

Fig. 7. Fluid inclusions in productive quartz of ore zone nos. 37 (a, b, d, e) and 1 (c, f) of Dvoinoe deposit.

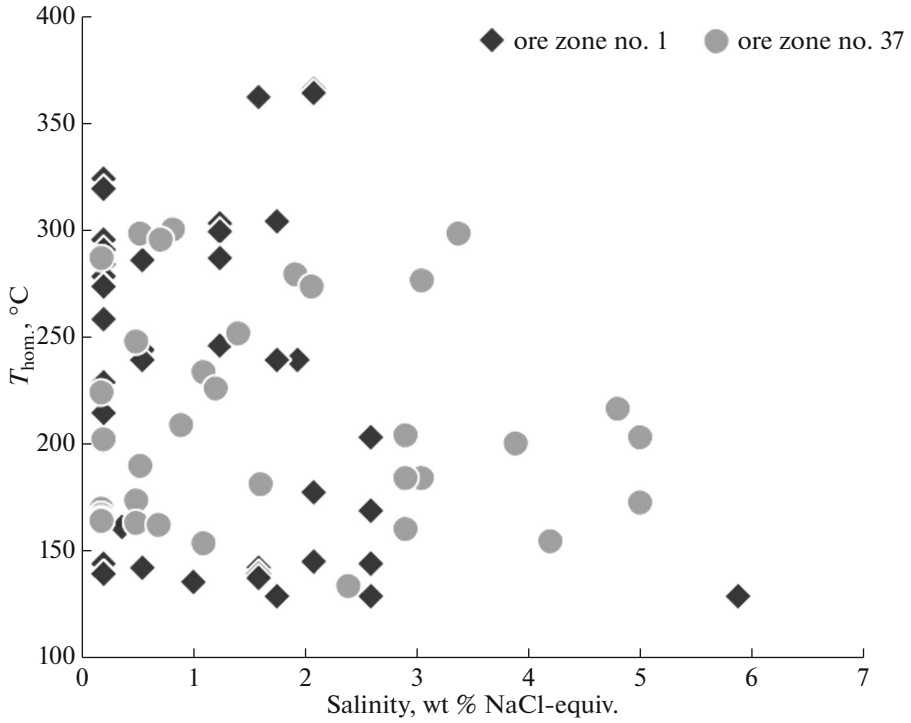

Fig. 8. Temperature vs. salinity for mineral-forming fluids of Dvoinoe epithermal deposit.

The fluid composition data are supplemented by bulk analysis of FIs from monofractions of three quartz samples from ore zone no. 37 with dominant primary FIs (Table 4, Fig. 10). These fluids contain H_2O, (g/kg H_2O) Cl (up to 1.5), hydrocarbon (8.7–4.6) and sulfate (up to 0.8) ions, Na (2.8–1.4), K (1.4–0.5), Ca (up to 0.13), and Mg (up to 0.11), which is consistent with cryometric data, as well as CO_2 (5.2–1.3), CH_4 (0.06–0.02), and the following trace elements (g/kg H_2O): Br (10.9–3.8), As (1095), Li (8.4–

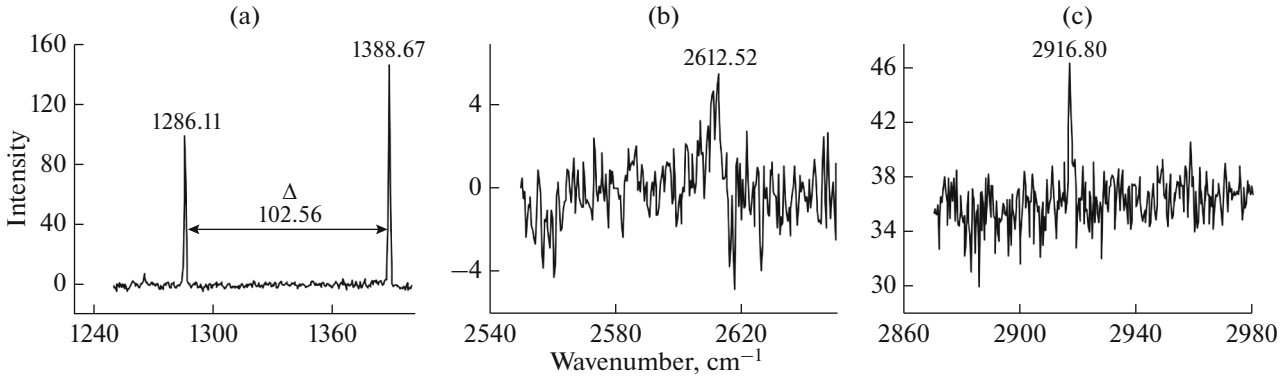

Fig. 9. Raman spectra of CO_2 (a), H_2S (b), and CH_4 (c) making up vapor phases of fluid inclusions in quartz of ores from Dvoinoe deposit (ore zone no. 37).

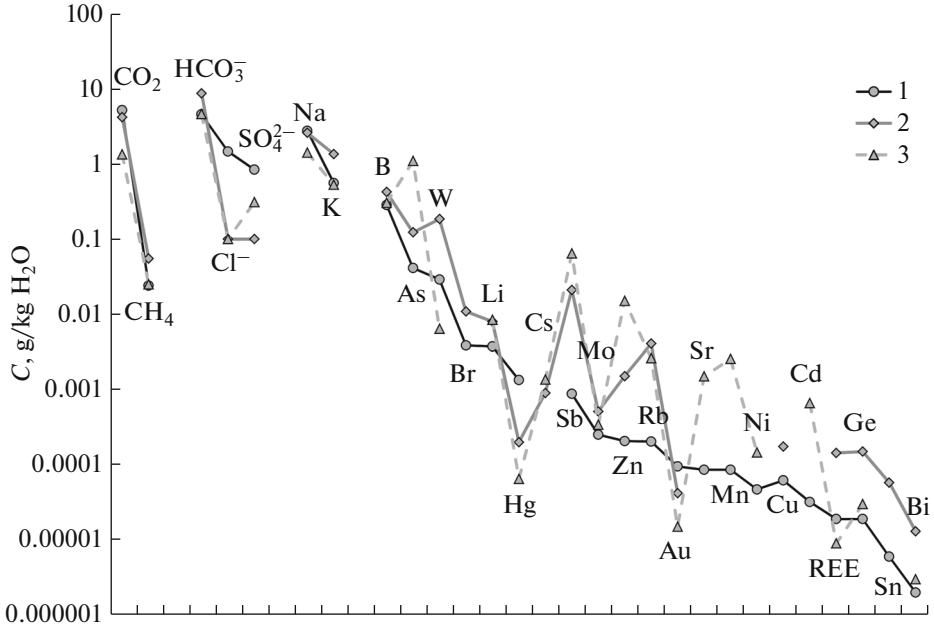

Fig. 10. Composition of mineral-forming fluids of Dvoinoe epithermal deposit (ore zone no. 37). (1–3) sample numbers (see Table 4); (1) DV-01; (2) DV-04; (3) DV-08.

3.7), B (424–284), Rb (4.1–0.2), Cs (1.4–0.9), Sr (1.5–0.05), Mo (0.5–0.3), Sb (64–0.9), Cu (0.2–0.06), Zn (15.1–0.2), Cd (0.7–0.03), Bi (0.01–0.002), Ge (0.15–0.02), Mn (2.6–0.09), Fe (up to 0.4), Co (up to 0.01), Ni (0.15–0.05), V (up to 0.08), Cr (up to 0.2), Y (0.02–0.01), Zr (0.17), Sn (0.06–0.01), Ba (up to 0.07), W (185–6.39), Au (0.095–0.015), Hg (1.4–0.07), Tl (0.02), and REEs (0.14–0.01). The main fluid composition indicators are as follows: CO_2/CH_4 = 217–53, Na/K = 5–2, and K/Rb = 2722–202.

GEOCHEMICAL FEATURES OF ORES

Ores from ore zone no. 37 of the Dvoinoe deposit mostly contain (wt %) SiO_2 (79.35–94.87) and noticeable amounts of Al_2O_3 (2.36–9.27) and K_2O (0.81–6.64), as well as MgO (0.20–2.04) and CaO (0.39–1.14) (Table 5). This means that the mineral composition of ores is dominated by quartz accompanied by adularia, carbonate, and hydromica. The ores are characterized by low and extremely low Na_2O, Fe_2O_3, TiO_2, P_2O_5, and MnO contents (Table 5). Judging from Table 5, the amount of sulfides in ores is very low (S_{total} varies from 0.13 to 0.56%), which supports the low-sulfide style of mineralization typical of ores of epithermal Au–Ag deposits.

The trace element composition of ores is shown in Table 6 and Fig. 11; it is normalized to the mean contents for the upper crust (Taylor and McLennan,

1988). The chondrite-normalized (Anders, 1989) REE patterns are shown in Fig. 12.

The ores are enriched in Au, Ag, As, Sb, Te, Cu, Zn, Pb, Cd, and Bi (Table 6, Fig. 11) relative to the mean values of the upper crust (Taylor and McLennan, 1988). The enrichment ratios vary from several times (Bi, Zn, Te) to tens (Pb, Cd, As, Cu), hundreds (Sb), thousands (Ag), and tens of thousands (Au) of times (Table 6; Fig. 11, indicating the geochemical similarity of some trace elements and their synchronous involvement in ore formation. The host volcanic rocks are enriched in Li, Rb, Tl, P, Sc, Ti, V, Mn, Sr, Co, Ba, and REEs relative to the mean values of the upper crust (Taylor and McLennan, 1988); however, the enrichment ratios for most elements are insignificant (2–5 times) (Tikhomirov et al., 2008, 2016; Sakhno et al., 2015).

As seen from Table 7, the REE patterns of ores are characterized by dominant light "hydrophile" REEs of the Ce group (Mineev, 1974; Zharikov et al., 1999). Host volcanic rocks are characterized by a similar REE composition (Tikhomirov et al., 2008, 2016; Sakhno et al., 2015). The U/Th ratio of ores (Table 7) of <0.75 (0.42–0.68) is evidence for their oxidative formation conditions (Jones and Manning, 1994). The Co/Ni ratio of ores (Table 7) of 0.52–1.2 is typical of mixing of medium- and low-temperature meteoric hydrothermal fluids and high-temperature magmatic fluid (Kun et al., 2014).

The ores are evidently enriched and depleted in LREE and HREE, respectively, with Hf/Sm, Nb/La, and Th/La ratios of <1 (Table 7). Thus, the ore-forming fluids belonged to a NaCl–H_2O hydrothermal system enriched in Cl relative to F (Oreskes and Einaudi, 1990), which agrees with an FI study in ore quartz (see below). The Y/Ho ratio of ores of 28.57–44.44 (Table 7) is similar to that of the present-day hydrothermal fluids of back-arc basins (Bau, 1991; Jones and Manning, 1994; Monecke et al., 2002).

The ores from the Dvoinoe deposit are characterized by low ΣREE contents (0.95–19.58 ppm) (Table 7). Similar low REE totals are typical of epithermal ores from the Kurama Ridge (Uzbekistan) and Banská-Stiavnica area (Slovakia) (Vinokurov et al., 1999). It should be noted that the ΣREE contents of ores (Table 7) are significantly lower than of host igneous and volcanic rocks of the OChVB (Tikhomirov et al., 2008, 2016; Sakhno et al., 2015). The chondrite-normalized REE contents of epithermal ores form weakly inclined patterns (Fig. 12) largely similar to those of host rocks (Tikhomirov et al., 2008, 2016; Sakhno et al., 2015) and are characterized by evident Eu minima (Fig. 12). Thus, it can be suggested that the host rocks of the OChVB could be sources of REEs and other trace elements for ore-forming fluids of the deposit.

The Eu and Ce anomalies are typically considered indicators of redox ore-formation conditions (Bortnikov et al., 2007; Goryachev et al., 2008). The

Table 4. Composition of solutions of fluid inclusions in quartz from ore veins of deposit

Element	DV-01	DV-04	DV-08
Major components, g/kg H_2O			
CO_2	5.19	4.18	1.34
CH_4	0.024	0.055	0.025
Cl^-	1.46	<0.2	<0.2
SO_4^{2-}	0.84	<0.2	0.63
HCO_3^-	4.56	8.72	4.61
Na	2.76	2.60	1.41
K	0.56	1.35	0.53
Ca	–	–	0.13
Mg	–	–	0.11
Trace elements, 10^{-3} g/kg H_2O			
Br	3.84	10.86	–
As	41.09	122.83	1094.56
Li	3.74	7.98	8.44
B	284.02	424.16	303.08
Rb	0.20	4.07	2.62
Cs	–	0.90	1.36
Sr	0.09	–	1.50
Mo	0.25	0.51	0.34
Sb	0.88	21.06	64.49
Cu	0.06	0.18	–
Zn	0.21	1.51	15.07
Cd	0.03	–	0.66
Bi	0.002	0.01	0.003
Ge	0.02	0.15	0.03
Mn	0.09	–	2.56
Fe	–	–	0.43
Co	–	–	0.01
Ni	0.05	–	0.15
V	–	0.76	–
Cr	–	0.18	–
Y	–	0.01	0.02
Zr	–	0.17	–
Sn	0.01	0.06	–
Ba	–	–	0.07
W	28.91	184.64	6.39
Au	0.095	0.042	0.015
Hg	1.35	0.20	0.07
Tl	–	0.02	0.02
REE	0.02	0.14	0.01
Na/K	5	2	3
CO_2/CH_4	217	76	53
K/Rb	2722	332	202

Table 5. Chemical composition of ores (wt %) from Dvoinoe deposit

Sample no.	SiO_2	TiO_2	Al_2O_3	Fe_2O_{3total}	MnO	MgO	CaO	Na_2O	K_2O	P_2O_5	S_{total}	Σ
308	93.37	0.03	2.36	0.17	0.01	0.20	0.39	0.10	0.81	0.02	0.15	97.61
141	80.52	0.14	8.91	0.80	0.05	1.81	0.77	0.17	6.22	0.05	0.46	99.90
113	92.13	<0.02	3.60	0.42	0.04	0.69	1.14	0.10	1.47	<0.02	0.13	99.72
240	94.87	<0.02	2.53	0.18	0.03	0.46	0.67	<0.10	0.85	<0.02	0.14	99.73
334	79.35	0.12	9.27	0.87	0.05	2.02	0.69	0.23	6.64	0.04	0.56	99.84
115	81.85	0.05	8.06	0.48	0.05	2.04	0.89	0.17	5.70	0.02	0.38	99.69
C_m	87.02	0.06	5.79	0.49	0.04	1.20	0.76	0.13	3.62	0.02	0.30	99.42

X-ray fluorescent (silicate) analysis, laboratory of IGEM RAS, analyst A.I. Yakushev.

Eu/Eu* and Ce/Ce* values of ores from the Dvoinoe deposit are negative and positive (close to 1), respectively (Table 7), indicating weakly oxidizing ore-formation conditions. The low Eu/Sm ratios (<1) of ores (Table 7) show their formation in the upper crustal level (Vinokurov, 1996).

DISCUSSION AND CONCLUSIONS

Two productive consecutive mineral assemblages (gold–pyrite and gold polysulfide) separated by tectonic movements have been identified as a result of a mineralogical study of ores from the Dvoinoe deposit

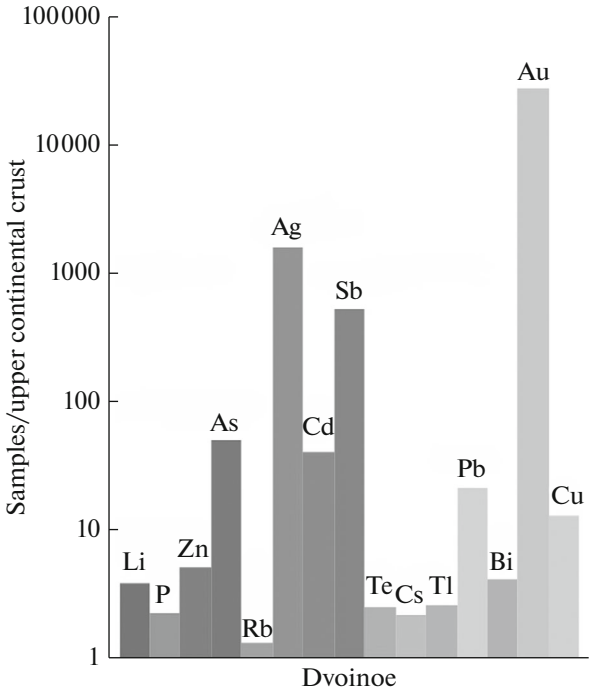

Fig. 11. Main trace element pattern of epithermal ores from Dvoinoe Au–Ag deposit (ore zone no. 37) normalized to mean values for upper crust (Anders, 1989).

(Table 8). Au-bearing pyrite of an early assemblage underwent cataclasis with the formation of small fractures and small clasts cemented by intimately intergrown minerals of the polysulfide assemblage. A minor amount of Ag minerals in ores indicates their Au mineral subtype (Sidorov, 1978).

The ores from the deposit differ from those of the Kupol deposit (Savva et al., 2012) by smaller grain sizes of of ore minerals and lower sulfidity. The high Au/Ag ratio (1 : 1 to 1 : 2) of ores from the Dvoinoe deposit are caused by Au/Ag ratio of electrum and low-fineness gold accompanied by a small amount of Ag from fahlore, hessite, and acanthite (Table 2). The ores from the Dvoinoe and Sentyabr'sky deposits (Savva et al., 2016) are similar in the presence of hessite, low Ag content of fahlore (mostly tennantite–tetrahedrite), the absence of arsenopyrite and Sb–As–Ag sulfosalts, and ore-formation temperature.

The Au/Ag, Te/Se, Rb/Sr, Th/La, Y/Ho, and U/Th ratios of ores from Early Cretaceous (Sentyabr'sky, Dvoinoe) and Late Cretaceous (Kupol, Moroshka) deposits differ (Table 7). The ores from the Dvoinoe deposit are characterized by a low ΣREE content; negative Eu anomaly (Eu/Eu < 1); low As, Sb, and Ag contents; and high Cu, Pb, and Zn contents (Tables 6, 7). The geochemical features are consistent with the mineral composition of ores. The high Rb/Sr, Th/La, Y/Ho, and U/Th ratios are most likely caused by the position of the deposit in the zone of influence of the Ilirnei granitic pluton.

An FI study showed that the ores from the deposit formed from weakly saline hydrothermal Na-, K, and Mg-bearing fluids with minor amounts of CO_2, HS^-, and CH_4 diluted by meteoric waters at decreasing temperatures from 370 to 130°C. These conditions are most favorable for the deposition of minerals and precipitation of Au and Ag (André-Mayer et al., 2002; Borovikov et al., 2009). The parameters and composition of ore-forming fluids of the Dvoinoe and Kupol deposits are similar except for the presence of noticeable sulfates in the ore-forming fluid of the Kupol deposit (Prokofiev et al., 2012; Volkov et al., 2012).

Table 6. Trace element composition of ores from Dvoinoe, Sentyabr'sky, Kupol, and Moroshka deposits

Element	Dvoinoe								Sentyabr'sky	Kupol	Moroshka
	Mean element contents, ppm						C_m	K_e			
	308	141	113	240	334	115			K_e (5)	K_e (5)	K_e (6)
Au	71.09	14.12	49.87	42.32	25.81	104.10	51.22	28455	256516	37758	46907.7
Ag	21.00	25.00	193.00	157.00	32.00	50.00	79.67	1593.3	830.0	3080.0	3112.0
Cu	240.00	180.00	430.00	300.00	350.00	470.00	328.33	13.13	83.9	1.3	9.0
Mo	0.11	0.72	1.10	0.18	0.30	0.02	0.40	0.27	0.8	5.8	27.5
Pb	311.00	142.00	291.00	477.00	231.00	1180.0	438.67	21.93	1262.2	3.8	51.9
Zn	209.00	101.00	280.00	605.00	109.00	877.00	363.50	5.12	235.1	0.9	19.6
Cd	2.90	1.10	3.30	6.10	1.40	9.10	3.98	40.65	2275.5	2.2	316.6
In	<bdl	<bdl	<bdl	<bdl	<bdl	<bdl	0.00	0.00	17.4	2168.3	0.0
Bi	2.50	0.29	0.15	0.19	0.05	0.06	0.54	4.25	0.6	0.3	1.4
As	30.00	24.00	137.00	97.00	85.00	80.00	75.50	50.33	47.7	137.8	890.9
Sb	46.00	72.00	193.00	158.00	88.00	83.00	106.67	533.33	122.5	1976.7	785.0
Sn	<bdl	1.00	0.18	0.39	2.90	1.40	0.98	0.18	0.3	0.2	0.4
W	<bdl	<bdl	0.85	0.09	0.27	<bdl	0.20	0.10	0.8	6.2	0.4
Tl	0.28	3.50	0.67	0.41	3.80	3.20	1.98	2.64	1.4	1.9	1.9
Te	0.90	3.80	5.50	18.00	5.00	2.50	5.95	2.55	1.7	0.1	3.9
Se	16.00	13.00	15.00	<bdl	<bdl	<bdl	7.33	0.15	0.1	0.6	0.0
Mn	64.00	310.00	259.00	181.00	285.00	274.00	228.83	0.38	1.2	1.4	1.4
Co	1.10	2.40	0.43	0.24	1.70	0.78	1.11	0.11	0.8	0.5	0.3
Ni	1.50	2.80	0.83	<bdl	1.70	0.65	1.25	0.06	0.2	0.2	0.1
Li	137.00	71.00	72.00	63.00	58.00	63.00	77.33	3.87	2.9	5.4	5.6
Rb	34.00	290.00	63.00	39.00	268.00	219.00	152.17	1.36	0.8	0.2	0.5
Be	0.61	0.89	0.87	1.20	0.79	0.59	0.83	0.28	0.2	0.3	0.3
P	4742.0	4729.00	<bdl	54.00	<bdl	<bdl	1587.50	2.27	0.5	1.2	1.1
Sc	11.00	17.00	<bdl	<bdl	0.13	<bdl	4.69	0.43	0.8	1.8	0.4
Ti	74.00	657.00	5.60	2.30	502.00	171.00	235.32	0.08	0.5	0.2	0.2
V	5.70	20.00	<bdl	<bdl	9.90	2.60	6.37	0.11	1.1	0.5	0.4
Cr	18.00	13.00	41.00	33.00	8.70	8.40	20.35	0.58	1.0	1.0	0.2
Ga	1.00	7.30	2.70	2.60	6.10	4.70	4.07	0.24	1.6	0.3	0.3
Sr	26.00	82.00	38.00	26.00	51.00	43.00	44.33	0.13	0.3	0.1	0.2
Y	1.00	3.80	0.32	0.10	2.40	1.20	1.47	0.07	0.3	0.3	0.2
Zr	5.10	29.00	1.40	0.76	31.00	11.00	13.04	0.07	0.3	0.1	0.1
Nb	<bdl	0.90	<bdl	<bdl	1.00	0.15	0.34	0.01	0.1	0.0	0.0
Ta	<bdl	<bdl	<bdl	<bdl	0.06	<bdl	0.01	0.00	0.1	0.1	0.0
Cs	6.40	11.00	8.90	8.50	8.10	6.50	8.23	2.23	3.5	1.5	2.6
Ba	39.00	191.00	53.00	28.00	172.00	123.00	101.00	0.18	0.8	0.0	0.3
La	0.55	3.20	0.18	0.04	3.10	1.20	1.38	0.05	0.3	0.1	0.1
Ce	1.20	7.70	0.44	0.12	7.10	2.70	3.21	0.05	0.2	0.1	0.1
Pr	0.15	1.00	0.04	0.02	0.76	0.27	0.37	0.05	0.3	0.1	0.1
Nd	0.67	4.00	0.25	0.05	2.90	1.30	1.53	0.06	0.3	0.1	0.1
Sm	0.16	0.79	0.03	0.04	0.56	0.22	0.30	0.07	0.3	0.1	0.2
Eu	0.01	0.18	0.00	0.00	0.11	0.05	0.06	0.07	0.5	0.3	0.4
Gd	0.22	1.00	0.01	0.69	0.17	0.25	0.39	0.10	0.3	0.2	0.2

Table 6. (Contd.)

Element	Dvoinoe								Sentyabr'sky	Kupol	Moroshka
	Mean element contents, ppm						C_m	K_e			
	308	141	113	240	334	115			K_e (5)	K_e (5)	K_e (6)
Tb	<bdl	0.10	<bdl	<bdl	0.08	0.03	0.03	0.05	0.3	0.2	0.2
Dy	0.11	0.65	0.03	<bdl	0.46	0.21	0.24	0.07	0.3	0.2	0.2
Ho	<bdl	0.11	<bdl	<bdl	0.08	0.03	0.04	0.05	0.3	0.2	0.2
Er	0.04	0.40	0.01	<bdl	0.28	0.10	0.14	0.06	0.3	0.2	0.2
Tm	<bdl	0.03	<bdl	<bdl	0.03	0.00	0.01	0.03	0.3	0.2	0.1
Yb	0.08	0.39	0.01	<bdl	0.31	0.11	0.15	0.07	0.3	0.2	0.2
Lu	<bdl	0.03	<bdl	<bdl	0.03	0.00	0.01	0.03	0.3	0.2	0.1
Hf	<bdl	0.39	<bdl	<bdl	0.63	0.08	0.18	0.03	0.3	0.1	0.1
Th	0.33	2.80	<bdl	<bdl	2.40	0.73	1.04	0.10	0.4	0.1	0.0
U	0.20	1.30	0.20	0.06	1.00	0.50	0.54	0.19	0.4	0.2	0.1

Bdl, below detection limit; C_m, mean arithmetic element content; K_e, coefficient of enrichment (C_m is normalized on mean contents of the upper crust after (Taylor and McLennan, 1988); 308, etc., sample numbers; (5) amount of samples. The contents of trace elements are analyzed using ICP MS, laboratory of IGEM RAS, analyst Ya.V. Bychkova; Au and Ag contents are determined using AAA, analyst V.A. Sychkova.

The high cooling rate of ore-forming fluid of the Dvoinoe deposit due to the contribution of cool meteoric waters could have caused the low degree of differentiation of ore material and the grain sizes of low-fineness gold, electrum, and sulfides. This regime is unfavorable for the formation of sulfosalts and incorporation of Sb and As into fahlore.

Our new mineralogical–geochemical data suggest that the Dvoinoe deposit, as well as the deposits of the Sentyabr'sky ore field (Savva et al., 2016), belongs to one large-scale ore-forming system related to K alkaline magmatism. In this case, these deposits can be considered zonally located toward the southeast from the center: first, Au–Pb–Zn (Sentyabr'sky), then Au–Ag (Dvoinoe). These data are important for regional forecasting metallogenic interpretations, prospecting, and evaluation of epithermal Au–Ag deposits.

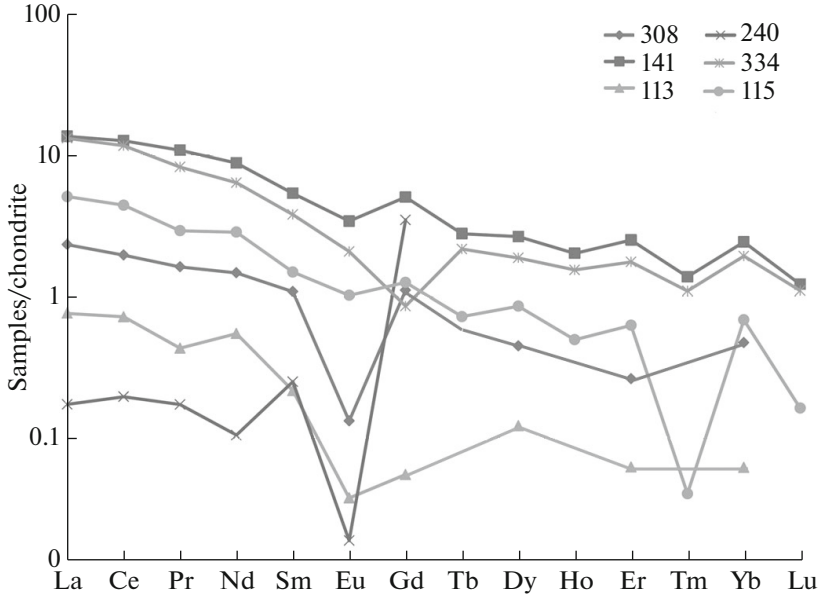

Fig. 12. Chondrite-normalized REE patterns of epithermal ores from Dvoinoe Au–Ag deposit (ore zone no. 37). 308, etc., sample numbers (see Table 6).

Table 7. Indicators of ores of Dvoinoe and adjacent epithermal deposits of OChVB

Indicators	Deposits									
	Dvoinoe							Sentyabr'sky	Kupol	Moroshka
	308	141	113	240	334	115	C_m	C_m (5)	C_m (5)	C_m (6)
∑REE	3.19	19.58	1.01	0.95	15.97	6.47	7.9	37.6	17.9	19.0
∑LREE	2.74	16.87	0.94	0.26	14.53	5.74	6.8	33.5	15.0	16.1
∑HREE	0.45	2.71	0.06	0.69	1.44	0.73	1.0	4.1	2.9	2.9
∑LREE/∑HREE	6.11	6.22	15.48	0.38	10.12	7.89	7.7	7.1	10.8	5.0
Hf/Sm	–	0.49	–	–	1.13	0.38	0.3	0.9	0.3	0.3
Nb/La	–	0.28	–	–	0.32	0.13	0.1	0.3	0.0	0.1
Th/La	0.60	0.88	–	–	0.77	0.61	0.5	0.4	0.1	0.1
Y/Ho	–	34.55	–	–	28.57	44.44	17.9	28.9	32.7	36.6
U/Th	0.61	0.46	–	–	0.42	0.68	0.4	0.5	0.9	0.8
Rb/Sr	1.31	3.54	1.66	1.50	5.25	5.09	3.1	0.7	0.6	1.2
Sr/Ba	0.67	0.43	0.72	0.93	0.30	0.35	0.6	0.8	1.5	2.4
Zr/Hf	–	74.36	–	–	49.21	132.53	42.7	36.0	5.2	7.6
Nb/Ta	–	–	–	–	18.18	–	3.0	9.7	1.5	4.2
Co/Ni	0.73	0.86	0.52	–	1.00	1.20	0.7	1.2	0.7	1.5
Te/Se	0.06	0.29	0.37	–	–	–	0.1	0.9	0.0	0.0
Au/Ag	3.39	0.56	0.26	0.27	0.81	2.08	1.2	9.2	0.5	0.5
Eu/Eu*	–	0.84	–	–	0.73	0.90	0.4	1.2	0.9	1.4
Ce/Ce*	1.03	1.17	1.24	0.99	1.16	1.14	1.1	1.0	1.0	0.9
LaN/YbN	4.92	5.57	12.23	–	6.79	7.41	6.2	8.0	5.8	6.0
LaN/SmN	2.15	2.53	3.51	0.69	3.46	3.41	2.6	3.2	2.6	2.8
GdN/YbN	2.34	2.07	0.89	–	0.44	1.84	1.3	1.7	1.8	1.8
LaN/LuN	–	11.07	–	–	11.92	31.14	9.0	7.5	1.9	8.0
ΣCe	2.57	15.90	0.91	0.23	13.86	5.47	6.5	31.7	14.1	14.9
ΣY	0.50	2.83	0.08	0.73	1.46	0.79	1.1	4.4	2.7	3.2
ΣSc	0.12	0.82	0.02	–	0.62	0.21	0.3	1.4	1.0	0.8
Eu/Sm	0.04	0.23	0.06	0.03	0.20	0.25	0.1	0.4	0.3	0.5
Ce/Yb	15.79	19.74	44.00	–	22.90	24.55	21.2	23.4	20.9	16.3
Eu/Ce	0.01	0.02	0.00	0.01	0.02	0.02	0.0	0.0	0.1	0.1

$Eu/Eu^* = Eu_N/(Sm_N*(Tb_N*Eu_N)^{1/2})^{1/2}$; $Ce/Ce^* = Ce_N/((2La_N + Sm_N)/3)$; LREES, light REEs; HREEs, heavy REEs; content sums by REE groups (Mineev, 1974): Ce, ΣCe; Y, ΣY; Sc, ΣSc.

ACKNOWLEDGMENTS

This work was supported by the Presidium of the Russian Academy of Sciences (program no. 4 "Deposits of Strategic Materials of Russia: Innovative Approaches to their Prediction, Assessment, and Exploration), the Russian Science Foundation (project no. 14-17-00170), the Far East Branch of the Russian Academy of Sciences (program no. 15-I-2-038), and the Russian Foundation for Basic Research (project no. 16-05-00949 A). The authors thank the staff of the Dolgov Laboratory of Thermobarogeochemistry

Table 8. Schematic succession of mineral formation of Dvoinoe deposit

MINERAL	STAGE OF MINERALIZATION	
	Gold–pyrite	Gold–polysulfide
Epidote		
Pyrophyllite		
Quartz		
Adularia		
Chlorite		
Hydromica		
Calcite		
Ankerite		
Pyrrhotite		
Pyrite		
Marcasite		
Sphalerite		
Chalcopyrite		
Galena		
Fahlore		
Acanthite		
Hessite		
Goldfieldite		
Native gold		
Native silver		

Thickness of line corresponds to relative abundance of minerals.

(IGM SB RAS) for permitting studies on a Lab Ram HR spectrometer.

REFERENCES

Akinin, V.V., Tomson, B.T., and Polzunenkov, G.O., U-Pb and $^{40}Ar/^{39}Ar$ dating of magmatism and mineralization at the Kupol and Dvoinoe gold deposits, *Izotopnoe datirovanie geologicheskikh protsessov: novye rezul'taty, podkhody i perspektivy: Mater. VI Rossiiskoi konf. po izotopnoi geokhronologii* (Isotope Dating of Geological Processes: New results, Approaches, and Prospects), Sankt-Petersburg: IGGD RAN, 2015, pp. 19–21.

Anders, E., Abundances of the elements: meteoric and solar, *Geochim. Cosmochim. Acta,* 1989, vol. 53, pp. 197–214.

Andre-Mayer, A.S. and Bailly, J.L., Chauvet, A., et al., Boiling and vertical mineralization zoning: a case study from the Apacheta low-sulfidation epithermal gold-silver deposit, southern peru, *Mineral. Deposita,* 2002, vol. 37, no. 5, pp. 452–464.

Bau, M., Rare-earth element mobility during hydrothermal and metamorphic fluid-rock interaction and the significance of the oxidation state of europium, *Chem. Geol.,* 1991, vol. 93, pp. 219–230.

Bodnar, R.J. and Vityk, M.O., Interpretation of microtermometric data for H_2O–NaCl fluid inclusions, *Fluid Inclusions in Minerals: Methods and Applications,* Pontignano: Siena, 1994, pp. 117–130.

Borisenko, A.S., Cryometric study of salt composition of gas–liquid inclusions in minerals, *Geol. Geofiz.,* 1977, no. 8, pp. 16–27.

Borovikov, A.A., Lapukhov, A.S., Borisenko, A.S., and Seretkin, Yu.V., The Asachinskoe epihermal Au–Ag deposit in southern Kamchatka: physicochemical conditions of formation, *Russ. Geol. Geophys.,* 2009, vol. 50, no. 8, pp. 685–694.

Bortnikov, N.S., Geochemistry and origin of the ore-forming fluids in hydrothermal–magmatic systems in tectonically active zones, *Geol. Ore Deposits,* 2006, vol. 48, no. 1, pp. 1–22.

Bortnikov, N.S., Gamyanin, G.N., Vikent'eva, O.V., Prokof'ev, V.Yu., Alpatov, V.A., and Bakharev, A.G., Fluid Composition and Origin in the Hydrothermal System of the Nezhdaninsky Gold Deposit, Sakha (Yakutia), Russia, *Geol. Ore Deposits,* 2007, vol. 49, no. 2, pp. 87–146.

Brown, P., Flincor: a computer program for the reduction and investigation of fluid inclusion data, *Am. Mineral.,* 1989, vol. 74, pp. 1390–1393.

Goryachev, N.A., Vikent'eva, O.V., Bortnikov, N.S., Prokof'ev, V.Yu., Alpatov, V.A., and Golub, V.V. The

world-class Natalka gold deposit, Northeast Russia: REE patterns, fluid inclusions, stable oxygen isotopes, and formation conditions of ore, *Geol. Ore Deposits,* 2008, vol. 50, no. 5, pp. 362–390.

Kryazhev, S.G., Prokof'ev, V.Yu., and Vasyuta, Yu.V., Application of ICP-MS in analyzing composition of ore-forming fluids, *Vestn. Mosk. Gos. Univ., Ser. 4. Geol.,* 2006, no. 4, pp, 30–36.

Kun, L., Ruidong, Y., Wenyong, Ch., et al., Trace element and REE geochemistry of the Zhewang gold deposit, southeastern Guizhou Province, china, *Chin. J. Geochem.,* 2014, vol. 33, pp. 109–118.

Manning, D.A.C., Comparison of geochemical indices used for the interpretation of palaeoredox conditions in ancient mudstones, *Chem. Geol.,* 1994, vol. 111, pp. 111–129.

Mineev, D.A., *Lantanoidy v rudakh redkozemel'nykh i kompleksnykh mestorozhdenii* (Lanthanides in Ores of the Rare-Earth and Complex Deposits), Moscow: Nauka, 1974.

Monecke, T., Kempe, U., and Gotze, J., Genetic significance of the trace element content in metamorphic and hydrothermal quartz: a reconnaissance study, *Geotektonika,* 2002, vol. 202, pp. 709–724.

Nikolaev, Yu.N., Prokof'ev, V.Yu., Apletalin, A.V., Vlasov, E.A., Baksheev, I.A., Kal'ko, I.A., and Komarova, Ya.S., Gold–telluride mineralization of the Western Chukchi Peninsula, Russia: mineralogy, geochemistry, and formation conditions, *Geol. Ore Deposits,* 2013, vol. 55, no. 2, pp. 96–124.

Oreskes, N. and Einaudi, M.T., Origin of rare-earth element enriched hematite breccias at the Olympic Dam Cu-U-Au-Ag deposit, Roxby Downs, South Australia, *Econ. Geol.,* 1990, vol. 85, no. 1, pp. 1–28.

Prokof'ev, V.Yu., Volkov, A.V., Sidorov, A.A., Savva, N.E., Kolova, E.E., Uyutnov, K.V., and Byankin, M.A., Geochemical peculiarities of ore-forming fluid of the Kupol Au–Ag epithermal deposit (Northeastern Russia), *Dokl. Earth Sci.,* 2012, vol. 447, pp. 1310–1313.

Sakhno, V.G., Barinov, N.N., Karas, O.A., et al., Petrological-geochemical isotope criteria for prediction of large-volume gold–silver ore potential of the volcanic structures of the Chukotka sector of the Arctic Russian coast, 2015. http://www.ras.ru/FStorage/download.aspx?id=2104c42d-696d-4e2e-91e6-0e5d55f55ca2

Savva, N.E., Kolova, E.E., Fomina, M.I., et al., Gold–base metal mineralization in explosive breccias: mineralogical–genetic aspects (Sentyabr'skoe deposit, NE Chukotka), *Vestn. SVNTs DVO RAN,* 2016, no. 1, pp. 16–36.

Savva, N.E., Pal'yanova, G.A., Byankin, M.A., The problem of genesis of gold and silver sulfides and selenides in the Kupol deposit (Chukchi Peninsula, Russia), *Russ. Geol. Geophys.,* 2012, vol. 53, no. 5, pp. 457–466.

Sidorov, A.A., *Zoloto-serebryanaya formatsiya Vostochno-Aziatskikh vulkanogennykh poyasov* (Gold–Silver Formation of the East Asian Volcanogenic Belts), Magadan, 1978.

Teilor S.R. and S. M. McLennan, *The Continental Crust: its Composition and Evolution*, Oxford: Blackwell, 1985.

Tikhomirov, P.L., Kalinina, E.A., Kobayashi, K., et al., Late Mesozoic silicic magmatism of the north Chukotka area (NE Russia): age, magma sources, and geodynamic implications, *Lithos,* 2008, vol. 105, pp. 329–346.

Tikhomirov, P.L. Kalinina, E.A., Moriguti, T., et al., Trace element and isotopic geochemistry of Cretaceous magmatism in NE Asia: spatial zonation, temporal evolution, and tectonic controls, *Lithos,* 2016, vol. 264, pp. 453–471.

Vinokurov, S.F., Europium anomalies in ore deposits and their geochemical significance, *Dokl. Earth Sci.,* 1996, vol. 347, pp. 281–283.

Vinokurov, S.F., Kovalenker, V.A., Safonov, Yu.G., et al., REE in quartz from epithermal gold deposits: distribution and genetic implications, *Geochem. Int.,* 1999, vol. 37, no. 2, pp. 145–152.

Volkov, A.V., Goncharov, V.I., and Sidorov, A.A., *Mestorozhdeniya zolota i serebra Chukotki* (Gold and Silver Deposits of Chukotka), Magadan: SVKNII DVO RAN, 2006.

Volkov, A.V., Prokof'ev, V.Yu., Savva, N.E., Sidorov, A.A., Byankin, M.A., Uyutnov, K.V., and Kolova, E.E., Ore Formation at the Kupol epithermal gold–silver deposit in Northeastern Russia deduced from fluid inclusion study, *Geol. Ore Deposits,* 2012, vol. 54, no. 4, pp. 295–303.

Zharikov, V.A., Gorbachev, N.S., Latfutt, P., et al., Rare earth element and yttrium distribution between fluid and basaltic melt at pressures of 1–12 kbar: evidence from experimental data, *Dokl. Earth Sci.,* 1999, vol. 366, pp. 543–545.

Translated by I. Melekestseva